Journal of Magnetic Resonance **136,** 169–175 (1999)
Article ID jmre.1998.1656, available online at http://www.idealibrary.com on IDEAL®

Quantitative Measurement of Transverse and Longitudinal Cross-Correlation between ^{13}C–^{1}H Dipolar Interaction and ^{13}C Chemical Shift Anisotropy: Application to a ^{13}C-Labeled DNA Duplex

Chojiro Kojima,* Akira Ono,† Masatsune Kainosho,† and Thomas L. James*,[1]

*Department of Pharmaceutical Chemistry, University of California, San Francisco, CA 94143-0446; and †Department of Chemistry, Faculty of Science, Tokyo Metropolitan University, Hachioji, Tokyo 192-03, Japan

Received June 8, 1998; revised November 6, 1998

Measurement of both longitudinal and transverse relaxation interference (cross-correlation) between ^{13}C chemical shift anisotropy and ^{13}C–^{1}H dipolar interactions is described. The ratio of the transverse to longitudinal cross-correlation rates readily yields the ratio of spectral densities $J(0)/J(\omega_C)$, independent of any structural attributes such as internuclear distance or chemical shift tensor. The spectral density at zero frequency $J(0)$ is also independent of chemical exchange effects. With limited internal motions, the ratio also enables an accurate evaluation of the correlation time for overall molecular tumbling. Applicability of this approach to investigating dynamics has been demonstrated by measurements made at three temperatures using a DNA decamer duplex with purines randomly enriched to 15% in ^{13}C. © 1999 Academic Press

Key Words: **molecular motion; spectral density analysis; correlation time.**

INTRODUCTION

Heteronuclear NMR techniques developed in the last decade enable more accurate determination of the frequency and amplitude of overall molecular tumbling and internal fluctuations, especially for proteins (*1–5*). These techniques are based primarily on ^{1}H-detected $^{15}N/^{13}C/^{2}H$ relaxation analysis and are also applicable to nucleic acids, although ^{13}C and ^{15}N chemical shift anisotropy (CSA) values of some nucleic acid residues are still unknown. Recently, transverse relaxation interference (cross-correlation) between the ^{15}N CSA and ^{15}N–^{1}H dipolar interactions of peptide backbone amides has been quantitatively measured, and this cross-correlation was demonstrated to be directly proportional to the generalized order parameter S^2 (*6*) However, in principle, the strength of the relaxation interference depends on the angles between the unique axes of the CSA and dipolar tensors, so neither CSA values nor values of the spectral density $J(\omega)$ are determined from such transverse cross-correlation experiments. As we demonstrate here, measurement of the longitudinal cross-correlation rate can be readily carried out and, in combination with the transverse cross-correlation rate, can be useful for elucidating $J(0)$ without exchange effects and, in the case of minimal internal motions, determining the overall tumbling correlation time. Specifically, the longitudinal and transverse cross-correlation rates for ^{13}C CSA and ^{13}C–^{1}H dipolar interactions in a DNA decamer duplex have been measured and reported here.

MEASUREMENT OF DD–CSA CROSS-CORRELATION

Relaxation interference between the ^{13}C CSA and ^{13}C–^{1}H dipole–dipole (DD) interactions results in the two ^{13}C–{^{1}H} doublet components differing in both the transverse and longitudinal relaxation rates (*6–8*). The ^{13}C cross-correlation rates are given by

$$R(^{13}C_X \rightarrow 2\,^{13}C_X\,^{1}H_Z) = 2\alpha d\{4J(0) + 3J(\omega_C)\} \quad [1.1]$$

$$R(^{13}C_Z \rightarrow 2\,^{13}C_Z\,^{1}H_Z) = 2\alpha d\{6J(\omega_C)\}, \quad [1.2]$$

where $\alpha = -2B_0 r_{CH}^3/(3h\gamma_H) \times f(\sigma_X, \sigma_Y, \sigma_Z)$, $d = h^2\gamma_H^2\gamma_C^2/(5r_{CH}^6)$, and $f(\sigma_X, \sigma_Y, \sigma_Z) = [\sigma_X(3\cos^2\theta_X - 1) + \sigma_Y(3\cos^2\theta_Y - 1) + \sigma_Z(3\cos^2\theta_Z - 1)]/2$. γ_i is the gyromagnetic ratio of spin i, r_{CH} is the distance between ^{1}H and ^{13}C nuclei, B_0 is the magnetic field strength, ω_C is the carbon Larmor frequency, σ_i is the ith principal component of the chemical shift tensor, and $\cos\theta_i$ is the direction cosine defining the orientation of the ^{13}C–^{1}H bond with respect to the ith axis of the ^{13}C chemical shift tensor. The coefficients α and d are not physical constants, because values for r_{CH}, σ_i and $\cos\theta_i$ are not constants (*9, 10*). It is apparent from Eqs. [1.1] and [1.2] that the ratio of spectral density values, $J(0)/J(\omega_C)$, is independent of the coefficients α and d and is determined from the two cross-correlation rates, $R(^{13}C_X \rightarrow 2\,^{13}C_X\,^{1}H_Z)$ and $R(^{13}C_Z \rightarrow 2\,^{13}C_Z\,^{1}H_Z)$, as

$$\frac{J(0)}{J(\omega_C)} = \frac{3}{4}\left(2\,\frac{R(^{13}C_X \rightarrow 2\,^{13}C_X\,^{1}H_Z)}{R(^{13}C_Z \rightarrow 2\,^{13}C_Z\,^{1}H_Z)} - 1\right). \quad [2]$$

[1] To whom correspondence should be addressed. E-mail: james@picasso.ucsf.edu.

1090-7807/99 $30.00

Unlike the typically measured transverse relaxation rate $R(^{13}C_X)$ or rotating frame relaxation rate, the transverse cross-correlation rate $R(^{13}C_X \rightarrow 2^{13}C_X\ ^1H_Z)$ is not affected by chemical exchange effects. Furthermore, $J(\omega_C)$ can be deduced by the full or reduced spectral density mapping procedure (*11–13*), so the true $J(0)$ value can be determined from Eq. [2]. The spectral density mapping procedures performed at one magnetic field strength can yield an apparent value for $J(0)$, but that value may contain contributions from chemical exchange; such chemical exchange contributions can be distinguished by carrying out measurements at several magnetic field strengths enabling the true $J(0)$ value to be determined (*11*). However, when only one or two magnetic fields are available, it would be much better to utilize Eq. [2] to determine the true $J(0)$.

If molecular tumbling is assumed isotropic, the correlation time is determined without any information about $J(\omega_C)$:

$$\tau = \frac{1}{\omega_C}\sqrt{\frac{J(0)}{J(\omega_C)} - 1} = \frac{1}{2\omega_C}\sqrt{6\,\frac{R(^{13}C_X \rightarrow 2^{13}C_X\ ^1H_Z)}{R(^{13}C_Z \rightarrow 2^{13}C_Z\ ^1H_Z)} - 7}\,. \qquad [3]$$

The equations above are also applicable to ^{15}N nuclei; the values or terms pertaining to ^{13}C, e.g., ω_C, $R(^{13}C_X \rightarrow 2^{13}C_X\ ^1H_Z)$, $R(^{13}C_Z \rightarrow 2^{13}C_Z\ ^1H_Z)$, are simply replaced by those for ^{15}N.

Pulse Schemes for Measurement of Cross-Correlation Rates

Figure 1 shows pulse schemes for quantitative measurement of transverse (upper) and longitudinal (lower) cross-correlation between ^{13}C–^1H dipolar coupling and ^{13}C CSA. The pulse sequence to record transverse CSA–DD cross-correlation rates of nitrogen, $R(^{15}N_X \rightarrow 2^{15}N_X\ ^1H_Z)$, reported previously (*6*) is identical to the upper sequence of Fig. 1 except for the gradient coherence selection with the sensitivity enhancement scheme (*14*), which is set for ^{13}C. The lower sequence is quite similar to the upper, although the ^{13}C magnetization relaxing during the cross-relaxation period 2Δ is longitudinal magnetization instead of transverse magnetization. Each pulse sequence is essentially a HSQC experiment with a transverse or longitudinal cross-relaxation period 2Δ inserted before the ^{13}C evolution period. To derive the longitudinal cross-correlation rate (lower pulse sequence), at least two independent measurements are required: the open ^1H 90° and composite $(90_y–220_x–90_y)$ 180° pulses are either applied (scheme A) or not applied (scheme B). The difference between scheme A and scheme B enables observation of cross-correlation effects during the period 2Δ. Likewise, at least two independent measurements are required to derive the transverse cross-correlation rate (upper pulse sequence).

In all schemes, ^1H magnetization is transferred to ^{13}C at time point a in Fig. 1. During the relaxation period 2Δ, the antiphase transverse (upper) or two-spin longitudinal (lower) magnetization relaxes at a rate $R(2^{13}C_Y\ ^1H_Z) \pm R(2^{13}C_Y\ ^1H_Z \rightarrow {}^{13}C_Y)$ or $R(2^{13}C_Z\ ^1H_Z) \pm R(2^{13}C_Z\ ^1H_Z \rightarrow {}^{13}C_Z)$, respectively. At time point b in Fig. 1, the transverse or longitudinal magnetization is given by

$$\begin{aligned}\sigma_b(\text{trans}) &= (C_YH_Z + C_Y/2)\exp[-2\Delta(R(2^{13}C_Y\ ^1H_Z) + R(2^{13}C_Y\ ^1H_Z \rightarrow {}^{13}C_Y))] \\ &\quad + (C_YH_Z - C_Y/2)\exp[-2\Delta(R(2^{13}C_Y\ ^1H_Z) - R(2^{13}C_Y\ ^1H_Z \rightarrow {}^{13}C_Y))] \\ &= C_YH_Z(\epsilon_X^+ + \epsilon_X^-) + C_Y(\epsilon_X^+ - \epsilon_X^-)/2 \qquad [4.1] \\ \sigma_b\,(\text{long}) &= (C_ZH_Z + C_Z/2)\exp[-2\Delta(R(2^{13}C_Z\ ^1H_Z) + R(2^{13}C_Z\ ^1H_Z \rightarrow {}^{13}C_Z))] \\ &\quad + (C_ZH_Z - C_Z/2)\exp[-2\Delta(R(2^{13}C_Z\ ^1H_Z) - R(2^{13}C_Z\ ^1H_Z \rightarrow {}^{13}C_Z))] \\ &= C_ZH_Z(\epsilon_Z^+ + \epsilon_Z^-) + C_Z(\epsilon_Z^+ - \epsilon_Z^-)/2, \qquad [4.2]\end{aligned}$$

where $\epsilon_X^\pm = \exp[-2\Delta(R(2^{13}C_X\ ^1H_Z) \pm R(^{13}C_X \rightarrow 2^{13}C_X\ ^1H_Z))]$ and $\epsilon_Z^\pm = \exp[-2\Delta(R(2^{13}C_Z\ ^1H_Z) \pm R(^{13}C_Z \rightarrow 2^{13}C_Z\ ^1H_Z))]$. Some relationships are used from the definition (*8*), $R(^{13}C_X \rightarrow 2^{13}C_X\ ^1H_Z) = R(^{13}C_Y \rightarrow 2^{13}C_Y\ ^1H_Z) = R(2^{13}C_Y\ ^1H_Z \rightarrow {}^{13}C_Y)$ and $R(^{13}C_Z \rightarrow 2^{13}C_Z\ ^1H_Z) = R(2^{13}C_Z\ ^1H_Z \rightarrow {}^{13}C_Z)$. With scheme A in Fig. 1, the ^1H 90° pulse just after time point b combined with the field gradient *g*4 destroys all two-spin order magnetization; thus at time point c, $\sigma_c(\text{trans}) = -C_Y(\epsilon_X^+ - \epsilon_X^-)/2$ and $\sigma_c(\text{long}) = -C_Y(\epsilon_Z^+ - \epsilon_Z^-)/2$. These in-phase components are converted to antiphase during the delay $2\tau = 1/(2\ ^1J_{CH})$, prior to $t1$ evolution. In scheme B, on the contrary, all magnetizations are maintained as at time point c, where $\sigma_c(\text{trans}) = -C_YH_Z(\epsilon_X^+ + \epsilon_X^-) - C_Y(\epsilon_X^+ - \epsilon_X^-)/2$ and $\sigma_c(\text{long}) = -C_YH_Z(\epsilon_Z^+ + \epsilon_Z^-) - C_Y(\epsilon_Z^+ - \epsilon_Z^-)/2$. After the period 2τ both the antiphase and in-phase terms remain unchanged, as the composite ^1H pulse is not applied in scheme B. Both terms are labeled at a ^{13}C frequency, and the antiphase magnetizations are refocused to the observable ^1H magnetization. However, the in-phase components are not refocused because they remain in-phase at the end of period $t1$. Thus, the ratio of the signal intensities obtained with schemes A and B becomes a simple function of the CSA-DD cross-correlation rates.

$$\begin{aligned}I_A/I_B\,(\text{trans}) &= (\epsilon_X^+ - \epsilon_X^-)/(\epsilon_X^+ + \epsilon_X^-) \\ &= \tanh(2\Delta R(^{13}C_X \rightarrow 2^{13}C_X\ ^1H_Z)) \qquad [5.1] \\ I_A/I_B\,(\text{long}) &= (\epsilon_Z^+ - \epsilon_Z^-)/(\epsilon_Z^+ + \epsilon_Z^-) \\ &= \tanh(2\Delta R(^{13}C_Z \rightarrow 2^{13}C_Z\ ^1H_Z)). \qquad [5.2]\end{aligned}$$

For both pulse sequences, intensity losses caused by other relaxation processes are identical in schemes A and B. During

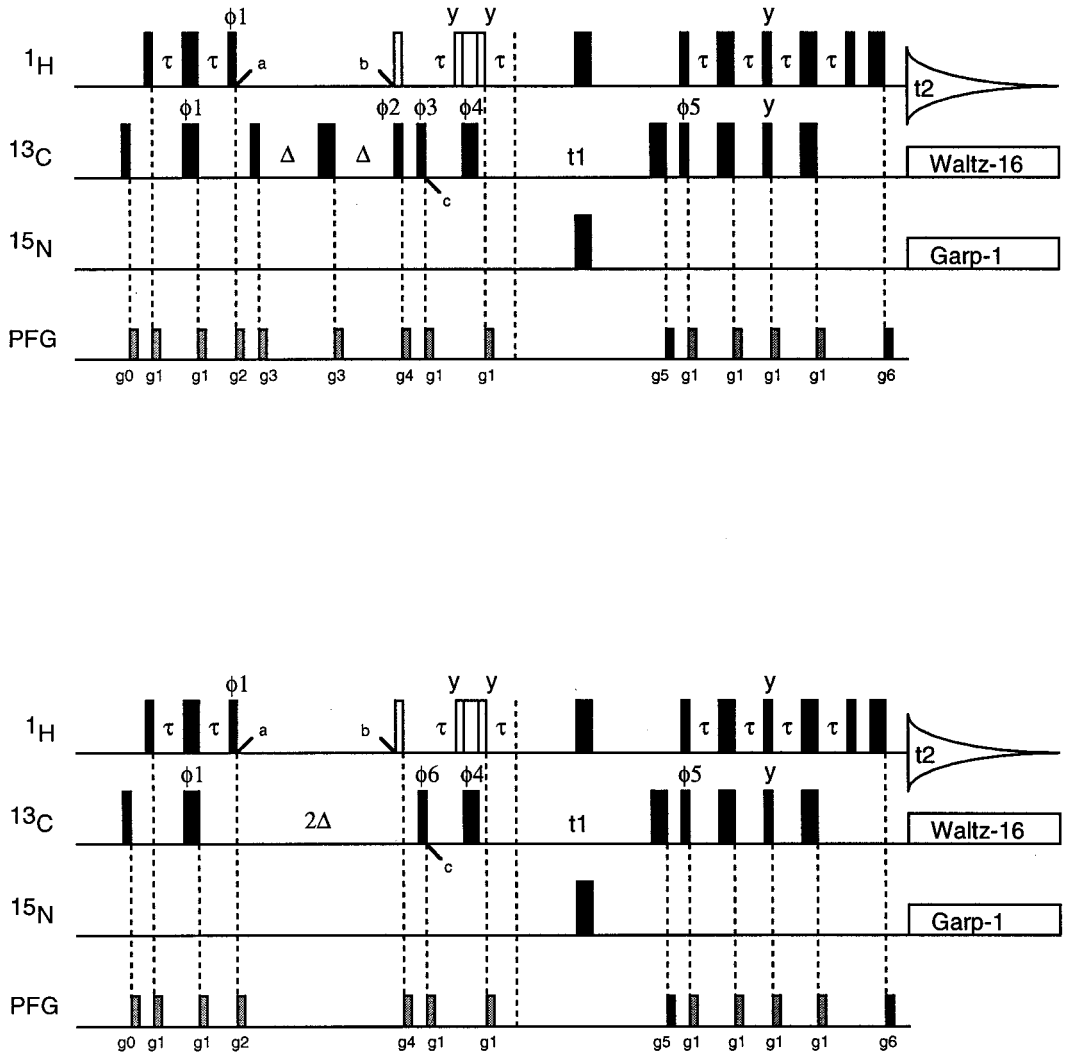

FIG. 1. Pulse schemes for quantitative measurements of transverse (upper) and longitudinal (lower) cross-correlation between ^{13}C–^{1}H dipolar coupling and ^{13}C chemical shift anisotropy. Narrow and wide pulses correspond to flip angles of 90° and 180°, respectively. For each upper and lower pulse sequence, At least two independent measurements are required to measure the transverse cross-correlation rate (upper pulse sequence) and two independent measurements are required to measure the longitudinal cross-correlation rate (lower pulse sequence): the open ^{1}H 90° and composite $(90_{y}–220_{x}–90_{y})$ 180° pulses are applied (scheme A) or not applied (scheme B). In scheme A, the experiments observe cross-correlation effects during the period 2Δ, and scheme B functions as the reference. The upper sequence is identical to that of a reported ^{15}N cross-correlation experiment (*6*) except the gradient coherence selection with sensitivity enhancement (*14*) is applied for ^{13}C. The lower sequence is quite similar to the upper though the ^{13}C magnetization during the cross-relaxation period 2Δ is longitudinal instead of transverse. Delay durations: $\tau = 1.19$ ms $(\frac{1}{4}\,{}^{1}J_{CH})$, $2\Delta = 15$, 30, and 60 ms (upper), or 60, 120, 180, and 240 ms (lower). Every pulse phase is x unless indicated. Phase cycling: $\phi1 = y, -y$; $\phi2 = 2(x), 2(-x)$; $\phi3 = x$; $\phi4 = 4(x), 4(y), 4(-x), 4(-y)$; $\phi5 = x$; $\phi6 = 2(x), 2(-x)$; Receiver $= x, 2(-x), x, -x, 2(x), -x$. Quadrature detection in the $t1$ dimension is achieved by alternation of $\phi5$ between x and $-x$ in concert with the polarity of the gradient $g6$, and additional 180° increment of $\phi3$ (or $\phi6$) and receiver by each $t1$ increment in the States–TPPI manner (*14, 24*). All gradients are rectangular. Gradients: $g0$ (5 G/cm, 0.5 ms); $g1$ (3 G/cm, 0.3 ms); $g2$ (8 G/cm, 1 ms); $g3$ (3 G/cm, 0.5 ms); $g4$ (7 G/cm, 1 ms); $g5$ (30 G/cm, 1 ms); $g6$ (30 G/cm, 0.25 ms).

the time period b to c (~1 ms) in Fig. 1, the $2C_ZH_Z$ term in scheme A relaxes faster than does C_Z in scheme B. However, the 1 ms duration is more than two orders of magnitude shorter than the inverse of the difference in relaxation rates of $2C_ZH_Z$ and C_Z, so the difference is negligible. In the transverse experiments (upper pulse sequence), any homonuclear ^{13}C–^{13}C scalar couplings may evolve during 2Δ. Such coupling will not affect the I_A/I_B ratio value, because scheme A and B each experience identical J coupling effects. However, the absolute value of the observed intensities I_A and I_B may change significantly depending on the magnitude of the J_{CC} coupling constants and the delay time 2Δ according to the function $\Pi_i(\cos \pi(nJ_{CC})_i 2\Delta)$, because the ^{13}C 90°_{X} pulse just after time point b combined with the field gradient $g4$ in Fig. 1 destroys all C_X and $2C_XH_Z$ magnetization generated by J_{CC} couplings. To avoid this problem, a more complicated pulse sequence is

required (*9*); otherwise the delay time 2Δ must be carefully chosen. It is noted that the I_A/I_B intensity ratio is independent of the J_{CC} coupling effects.

MATERIALS AND METHODS

The sample used here was a DNA decamer duplex in which every adenosine and guanidine is randomly fractionally enriched with 15% ^{13}C and 98% ^{15}N stable isotopes. The sequence *d*(CATTTGCATC) · *d*(GATGCAAATG) was selected because the solution structure of this oligomer has been well characterized (*15, 16*). Additionally, detailed ^{13}C relaxation studies in D_2O (*17*) and free molecular dynamics (MD) simulation analysis (*18*) have been done with this sequence recently. Details of the sample preparation were described in previous reports (*19*). The NMR sample contained 0.9 mM of double strand dissolved in 20 mM phosphate buffer containing 100 mM NaCl and 0.1 mM EDTA, adjusted to pH 6.8. The solvent was 90% H_2O and 10% D_2O. All NMR experiments were carried out on a Varian Inova-600 spectrometer operating at 600 MHz ^1H frequency, equipped with a pulsed field gradient $^1H/^{13}C/^{15}N$ triple-resonance probe head. Recorded matrices consisted of 128 ($t1$) × 1024 ($t2$) data points with acquisition times of 38 ($t1$) and 205 ms ($t2$). For scheme A (Fig. 1), 128 scans per FID were collected, whereas 32 scans were acquired for Scheme B. Other acquisition parameters were described in the legends of Fig. 1. All 2D spectra were processed on Sun Sparcstations or IRIS Indigo R5000 workstations using nmrPipe software (NIH, Bethesda) (*20*) and our home-written Sparky software (UCSF, San Francisco). Apodization consisted of a 90°-shifted sine-squared window function applied in the $t2$ dimension and a 90°-shifted sine function in the $t1$ dimension; data were zero-filled twice in each dimension prior to Fourier transformation. Intensities were taken from peak height measurements.

The longitudinal and transverse ^{13}C CSA and ^{13}C–^1H dipolar cross-correlation rates were determined from data acquired at three temperatures using the following 2Δ delay times: 30 ms (transverse, 10°C); 15, 30, 60, and 60 ms (transverse, 20°C); 15, 30, 30, and 60 ms (transverse, 30°C); 180 ms (longitudinal, 10°C); 60, 120, 180, and 240 ms (longitudinal, 20°C); 60, 120, 180, and 240 ms (longitudinal, 30°C). The expected J_{CC} coupling effects on the absolute intensity (*vide supra*) were not evident for our uniformly 15% ^{13}C enriched sample at either C8 or C2 positions. From Eqs. [5.1] and [5.2], a single 2Δ delay time is enough to determine a single cross-relaxation rate, e.g., the data at 10°C. At 20° and 30°C, three or four delay times were used to evaluate any dependence of the cross-relaxation rate on delay time 2Δ. The intensity I_A/I_B ratio values agree very well with the theoretical relations as a function of the delay time 2Δ shown in Eqs. [5.1] and [5.2]. That means there is no significant second-order effect on the I_A/I_B ratio throughout the whole 2Δ period, where the cross-correlation effects between a ^{13}C–^1H dipole and ^{13}C–^{13}C dipole could become observable.

The longitudinal and transverse ^{13}C relaxation rates $R(^{13}C_Z)$ and $R(^{13}C_X)$ were measured in a series of 2D heteronuclear ^{13}C–^1H correlated spectra using INEPT and reverse INEPT pulse sequences with a gradient sensitivity enhancement scheme (*14, 21*). For $R(^{13}C_X)$ measurements, the continuous-wave ^{13}C spin–lock sequence was employed instead of the Carr–Purcell–Meiboon–Gill pulse train, where the ^{13}C spin–lock pulse field strength was 2.3 kHz (90° pulse width ~110 μs). The Levenburg–Marquardt algorithm of KaleidaGraph 3.0 (Abelbeck Software) was used to extract the relaxation rate constants. Two parameter fitting ($y = Ae^{-Bx}$) was applied, assuming a monoexponential decay for cross-peak intensities. The pulse repetition time was 1.5 s, i.e., ~3 times ^{13}C T1, and the total acquisition time of each 2D spectrum was 3.5 and 1.7 h for $R(^{13}C_X)$ and $R(^{13}C_Z)$ experiments, respectively. Each relaxation data set was recorded with the following relaxation delay times: 50, 100, 150, 200, 250, 300, 400, and 500 ms for $R(^{13}C_Z)$ and 8, 16, 24, 40, 56, and 72 ms for $R(^{13}C_x)$. The total acquisition time for $R(^{13}C_X)$ and $R(^{13}C_Z)$ experiments was 1 day and $\frac{1}{2}$ day, respectively.

RESULTS AND DISCUSSION

The overall correlation time τ_c was determined by two different methods: by the ^{13}C T1/T2 ratio ($=R(^{13}C_x)/R(^{13}C_z)$) method and via Eq. [3]. As noted previously (*2*), for measurement of τ_c the T1/T2 ratio is assumed to be approximately independent of internal motion; of course, this is not always true for a flexible region of a molecule. The $J(0)/J(\omega_C)$ ratio method (Eq. [3]) can determine the overall correlation time only when internal motion is negligible. For the DNA decamer used here, $J(0)$ and $J(\omega_C)$ were dominated by the overall motion (*17*), so internal motion was neglected as a first approximation. The validity of this approximation will be evaluated later. The apparent correlation time was determined for each CH site of all purine bases by both methods, and then simply averaged over the nonterminal residues to estimate the overall correlation time. On the basis of our previous results (*17*), the overall tumbling was assumed to be isotropic rather than anisotropic and the terminal residues to be somewhat flexible.

In Table 1 the correlation times obtained are shown with observed transverse and longitudinal cross-correlation rates and the $J(0)/J(150)$ ($=J(0)/J(\omega_C)$) ratio value. Within the standard deviation of averaging, both methods give identical results at the three temperatures: 10, 20, and 30°C. This means the newly proposed $J(0)/J(\omega_C)$ method of Eq. [3] works very well for our DNA decamer molecule. We can first consider why the $J(0)/J(\omega_C)$ method is successful. In the plot of Fig. 2, the behavior of the $J(0)/J(150)$ ratio is depicted as a function of the correlation time, based on Eq. [3]. At a glance, the $J(0)/J(150)$ value increases steeply with the correlation time

TABLE 1

Transverse and Longitudinal Cross-Correlation Rates Measured at 14.1 T (600 MHz ^{1}H Frequency), Spectral Density Ratio, and Isotropic Correlation Times of a DNA Decamer Duplex at 10, 20 and 30°C[a]

	30°C	20°C	10°C
$R(^{13}C_X \rightarrow 2^{13}C_X\ ^1H_Z)$, s^{-1}	12.83 ± 2.50	16.70 ± 2.87	26.75 ± 5.52
$R(^{13}C_Z \rightarrow 2^{13}C_Z\ ^1H_Z)$, s^{-1}	1.92 ± 0.30	1.64 ± 0.26	1.64 ± 0.24
$J(0)/J(150)$	9.24 ± 0.77	14.70 ± 2.18	24.03 ± 4.95
τ_c(CSA–DD), ns	3.02 ± 0.14	3.89 ± 0.32	5.03 ± 0.56
τ_c(T1/T2), ns	2.86 ± 0.21	3.81 ± 0.33	5.25 ± 0.73

[a] Each value is the average over all C8–H8 and C2–H2 positions, except terminal residues, together with standard deviations on averaging. $R(^{13}C_X \rightarrow 2^{13}C_X\ ^1H_Z)$ and $R(^{13}C_Z \rightarrow 2^{13}C_Z\ ^1H_Z)$ are the observed transverse and longitudinal CSA–DD cross-correlation rates, respectively. $J(0)/J(150) = (3/4)[2 \times R(^{13}C_X \rightarrow 2^{13}C_X\ ^1H_Z)/R(^{13}C_Z \rightarrow 2^{13}C_Z\ ^1H_Z) - 1]$ is a ratio of spectral density function values at 0 and 150 MHz. τ_c(CSA–DD) and τ_c(T1/T2) are the isotropic correlation times, respectively determined from the CSA–DD cross-correlation rates (Eq. [3]) and by the T1/T2 ratio assuming no internal motion.

increase. This is because the $J(0)/J(150)$ ratio value is roughly proportional to the square of the correlation time (see Eq. [3]). The parabolic relationship shown here reduces the error in the correlation time due to the experimental error of the observed $R(^{13}C_X \rightarrow 2^{13}C_X\ ^1H_Z)/R(^{13}C_Z \rightarrow 2^{13}C_Z\ ^1H_Z)$ ratio; there is a reduction by a factor of about two as a relative error estimated by simple error propagation. Our DNA decamer results are illustrated in the lower panel of Fig. 2. It is noted that the T1/T2 ratio method also has a quite similar parabolic relation, so this merit is not limited to the $J(0)/J(\omega_C)$ ratio method.

If there was any effect of chemical exchange on ^{13}C relaxation, the ^{13}C T2 value would be shortened and the T1/T2 ratio consequently increased. However, the $J(0)/J(\omega_C)$ ratio method is completely independent of such chemical exchange effects. As shown in Table 1, both the T1/T2 and $J(0)/J(\omega_C)$ methods give identical correlation times, so it may be concluded that there are no or negligible chemical exchange effects on the correlation time value derived. However, it is not safe to conclude there is no chemical exchange effect on ^{13}C T2 because of the following. The presence of a fast internal motion contributes to a $J(0)$ value decrease, but a chemical exchange effect works in the opposite way. As a result, the apparent $J(0)$ may not change much, so the T1/T2 ratio method may not be very sensitive to chemical exchange. In fact a small (<3 Hz) but explicit effect of chemical exchange was found to be necessary to explain our ^{13}C relaxation data in D_2O (*17*); the work reported in this paper has been done in H_2O and could differ due to chemical exchange entailing exchangeable protons.

Internal motion clearly decreases the $J(0)/J(150)$ ratio values. Such internal motion effects may be considered in the context of the Lipari–Szabo model-free formalism (*22*). From our previous motional analysis of this oligomer, the generalized order parameter S^2 and the internal motion correlation time are determined to be 0.8 ± 0.1 and 0.02 ± 0.02 ns, respectively (*17*). Figure 3 shows the normalized $J(0)/J(150)$ ratio values as a function of the generalized order parameter S^2, where each $J(0)/J(150)$ ratio value is normalized by the value obtained without internal motion. In the upper plots, the internal motion correlation time is maintained at 0.02 ns but the overall correlation time τ_c is changed from 0.5 to 20 ns. For a particular S^2 value, the accuracy of the overall correlation time determination clearly bceomes more sensitive to $J(0)/J(150)$ ratio errors as the correlation time increases. However, even at $S^2 = 0.6$ and $\tau_c = 20$ ns, the relative error in τ_c does not exceed more than 20%; this is due to the very fast internal motion assumed here. In the lower plots of Fig. 3 the overall

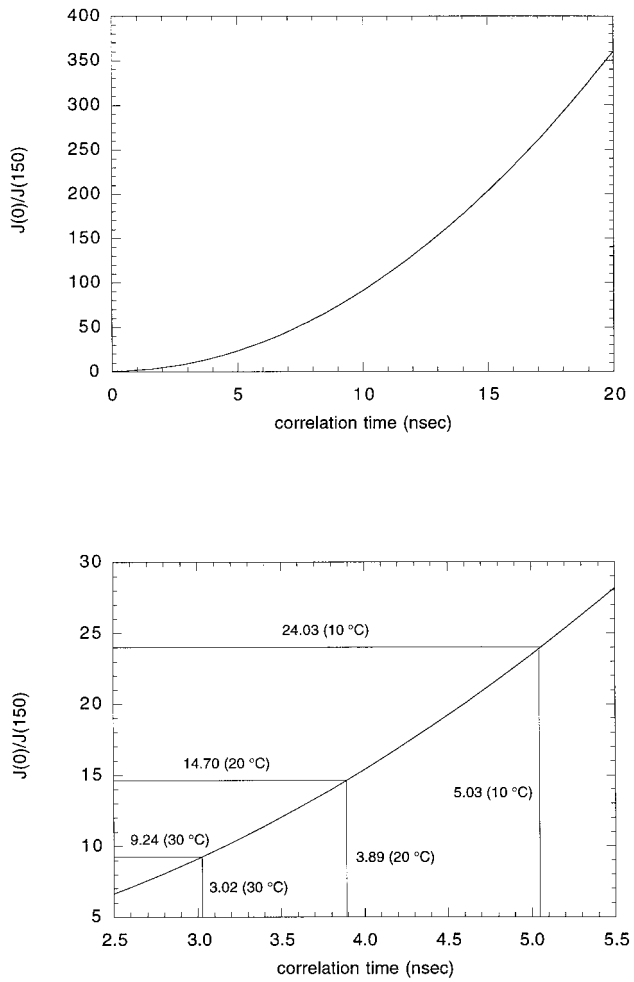

FIG. 2. The relationship between the $J(0)/J(150)$ ratio and the correlation time assuming the isotropic overall tumbling with no internal motion. $J(0)/J(150) = (2\pi \times 150\ \text{MHz})^2 \times (\text{correlation time})^2 + 1$, where $J(0)$ and $J(150)$ are the spectral density values at 0 and 150 MHz, respectively. The lower panel is an expanded part of the upper one, where experimental $J(0)/J(150)$ values for a DNA decamer duplex at 10°, 20°, and 30°C are presented with corresponding correlation times.

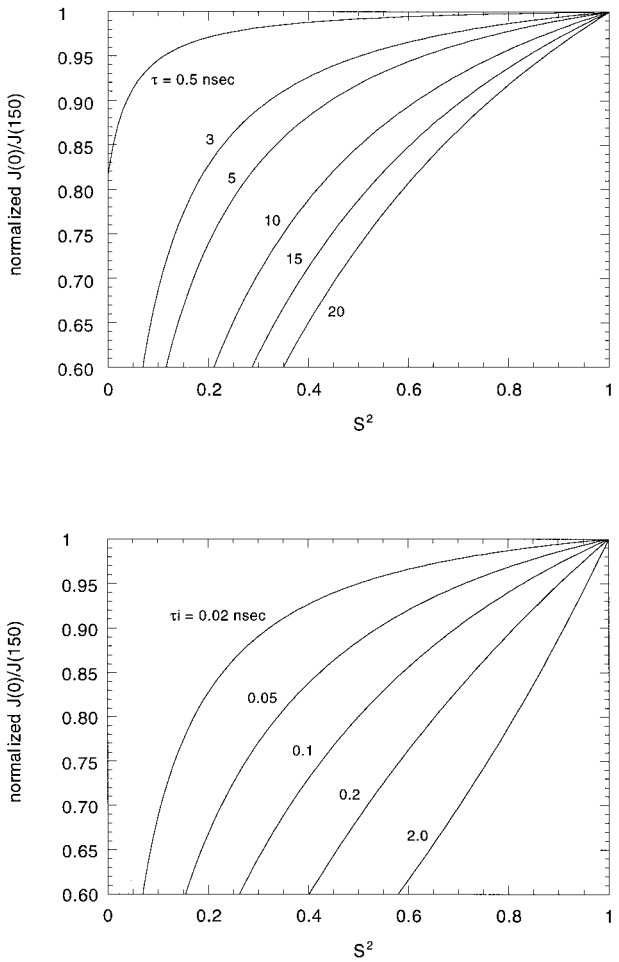

FIG. 3. The effect of internal motion on the $J(0)/J(150)$ ratio value as a function of the generalized order parameter S^2. The Lipari–Szabo model-free formalism is employed to assess the internal motion effects. In the upper plots the overall correlation time τ_c is changed from 0.5 to 20 ns, while the internal correlation time $\tau i = 0.02$ ns. In the lower plots the internal correlation time τ_i is changed from 0.02 to 2 ns, assuming the overall correlation time $\tau = 3.0$ ns. Each $J(0)/J(150)$ ratio value is normalized by the value obtained without internal motion.

correlation time is kept at 3.0 ns, but the internal motion correlation time τ_i is changed from 0.02 to 2 ns. The larger internal motion correlation times give steeper decreases in $J(0)/J(150)$ ratio values with S^2. If $S^2 = 0.6$ and $\tau_i = 2$ ns, the relative error in τ_c approaches nearly 40%. Considering both plots and our previous motional analysis in D_2O, it is evident that our calculated overall correlation time may be underestimated but by less than 5%. In general, when the amplitude of the internal motion and/or the internal motion correlation time is large, the $J(0)/J(150)$ ratio method should not be used to determine the overall correlation time because of the large error that arises from neglecting internal motion. In other words, if the internal motion correlation time is not fast enough, the $J(0)/J(150)$ ratio value leads to large systematic errors in the correlation time determined. This problem is not limited to the $J(0)/J(150)$ ratio method; the T1/T2 ratio method also has these demerits, so the problem is quite general. For larger molecules which may have slower overall and internal motions, the ^{15}N nucleus could be better than ^{13}C because $J(\omega_C)$ is more sensitive to internal motion than is $J(\omega_N)$ (*10*).

CONCLUSIONS

The longitudinal and transverse cross-correlation rates between the ^{13}C CSA and ^{13}C–^{1}H dipolar interactions of purines in a DNA duplex have been quantitatively measured. The ratio of the transverse and longitudinal cross-correlation rates, $R(^{13}C_X \rightarrow 2^{13}C_X^1H_Z)/R(^{13}C_Z \rightarrow 2^{13}C_Z^1H_Z)$, is theoretically related to the spectral density value ratio $J(0)/J(\omega_C)$ without dependence upon any structural or physical constants such as internuclear distance, Larmor frequency, or chemical shift tensor. Neglecting internal motion, the overall correlation times of the uniformly 15% ^{13}C-enriched DNA decamer are determined from the $J(0)/J(\omega_C)$ ratio values at three temperatures (10°, 20° and 30°C) in H_2O. The differences between the average correlation time values measured from the ^{13}C T1/T2 ratio and from the $J(0)/J(\omega_C)$ ratio are smaller than the standard deviation on averaging over all CH sites in the purine bases using either method. The $J(0)/J(\omega_C)$ ratio gives the correct correlation time neglecting the internal motion; this is due to the very fast internal motion and the relatively high order parameter values ($S^2 \sim 0.8$) of the DNA decamer duplex. The $J(0)/J(\omega_C)$ ratio values, which can be determined from two readily measured cross-correlation rates, should potentially give us more accurate information about molecular motions than we can obtain from ^{13}C T1, T2, NOE data. During the five-month initial review of our manuscript, a paper appeared which describes essentially the same approach for ^{15}N–^{1}H (*23*).

ACKNOWLEDGMENTS

We thank the Central Research Laboratories of Ajinomoto Co., Inc., for their assistance in preparing isotope-labeled adenosine and guanosine. This work was supported by Grant RG401/95 from the Human Frontier Science Program (Strasbourg, France) and Grant GM39247 from the National Institutes of Health to T.L.J., and by a grant from CREST (Core Research Evolutional Science and Technology) of Japan Science and Technology Corporation (JST) to M.K. C.K. was supported in part by a Toyobo Biotechnology Foundation and JSPS Fellowship.

REFERENCES

1. N. R. Nirmala and G. Wagner, *J. Am. Chem. Soc.* **110,** 7557–7558 (1988).
2. L. E. Kay, D. A. Torchia, and A. Bax, *Biochemistry* **28,** 8972–8979 (1989).
3. J. W. Peng and G. Wagner, *J. Magn. Reson.* **98,** 308–332 (1992).
4. D. R. Muhandiram, T. Yamazaki, B. D. Sykes, and L. E. Kay, *J. Am. Chem. Soc.* **117,** 11536–11544 (1995).
5. A. G. Palmer, III, *Curr. Opin. Struct. Biol.* **7,** 732–737 (1997).

6. N. Tjandra, A. Szabo, and A. Bax, *J. Am. Chem. Soc.* **118,** 6986–6991 (1996).
7. M. Guéron, J. L. Leroy, and R. H. Griffey, *J. Am. Chem. Soc.* **105,** 7262–7266 (1983).
8. M. Goldman, *J. Magn. Reson.* **60,** 437–452 (1984).
9. N. Tjandra and A. Bax, *J. Am. Chem. Soc.* **119,** 9576–9577 (1997).
10. J. M. Schmidt, C. Ludwig, and H. Rüterjans, Abstract from Seventh Chianti Workshop on Magnetic Resonance: Nuclear and Electron Relaxation, San Miniato (Pisa, Italy), 1997.
11. J. W. Peng and G. Wagner, *Biochemistry* **34,** 16733–16752 (1995).
12. R. Ishima and K. Nagayama, *J. Magn. Reson. B* **108,** 73–76 (1995).
13. N. A. Farrow, O. Zhang, A. Szabo, D. A. Torchia, and L. E. Kay, *J. Biomolec. NMR* **6,** 153–162 (1995).
14. L. E. Kay, P. Keifer, and T. Saarinen, *J. Am. Chem. Soc.* **114,** 10663–10665 (1992).
15. K. Weisz, R. H. Shafer, W. Egan, and T. L. James, *Biochemistry* **31,** 7477–7487 (1992).
16. K. Weisz, R. H. Shafer, W. Egan, and T. L. James, *Biochemistry* **33,** 354–366 (1994).
17. C. Kojima, A. Ono, M. Kainosho, and T. L. James, *J. Magn. Reson.,* in press.
18. D. E. Konerding, T. E. Cheatham III, P. A. Kollman, and T. L. James, *J. Biomolec. NMR,* in press.
19. S. Tate, A. Ono, and M. Kainosho, *J. Am. Chem. Soc.* **116,** 5977–5978 (1994).
20. F. Delaglio, S. Grzesiek, G. W. Vuister, G. Zhu, J. Pfeifer, and A. Bax, *J. Biomolec. NMR* **6,** 277–293 (1995).
21. N. A. Farrow, R. Muhandiram, A. U. Singer, S. M. Pascal, C. M. Kay, G. Gish, S. E. Shelson, T. Pawson, J. D. Forman-Kay, and L. E. Kay, *Biochemistry* **33,** 5984–6003 (1994).
22. G. Lipari, and A. Szabo, *J. Am. Chem. Soc.* **104,** 4546–4559 (1982).
23. C. D. Kroenke, J. P. Loria, L. K. Lee, M. Rance, and A. G. Palmer, *J. Am. Chem. Soc.* **120,** 7905–7915 (1998).
24. D. Marion, M. Ikura, R. Tschudin, and A. Bax, *J. Magn. Reson.* **85,** 393–399 (1989).